JOURNAL OF MATERIALS SCIENCE 15 (1980) 139–148

Structural studies on the alloying behaviour of γ-Mn and the development of a high damping capacity in Mn-Cu alloys

P. VENKATESWARARAO, D. K. CHATTERJEE*
Defence Metallurgical Research Laboratory, Hyderabad, India

Quenched Mn–Cu alloys undergo an unusual type of phase transformation and form metastable structures. A miscibility gap exists in these alloys, and the stability of the alloy phases is associated with the allotropic form of elemental Mn-atoms beyond the equi-atomic compositions. Quenched Mn–33.4 at % Cu alloy, which corresponds to the centre of the miscibility gap, upon ageing gives rise to a high damping capacity. The internal lattice strain which is the cause of the high damping capacity is thought to be due to interfacial misfit of the MnCu phase and elemental Mn in the proposed metastable structure of the alloy.

1. Introduction

Quenched alloys in the Mn–Cu system in the composition range ~25 to 50 at% Cu are known to exhibit a high damping capacity. Alloys in this composition range are reported to have the f c c structure upon quenching from 800° C which readily transforms to f c t upon ageing at 400° C [1–5]. The high damping capacity in aged alloys is considered to be due to a tetragonality in the structure, and the movement of twin domain walls is thought to be a possible mechanism for energy dissipation. The above observations were based upon the f c t structure for γ-Mn; however, it has recently been reported that γ-Mn possess the b c t structure with two atoms per unit cell [6]. This difference in the crystal structure of Mn and Cu brings up an important consideration concerning the miscibility between these elements in the Mn–Cu system. The possible existence of a miscibility gap in this system [7] has been examined in the present study, and the results are presented herein. The present data on the miscibility gap based upon X-ray diffraction work was also compared with other published work. Measurements on the damping capacity of some of the compositions in this alloy system are also reported with a view to elucidating the possible mechanism responsible for the high damping capacity of these alloys.

2. Experimental procedure and results

Mn–Cu alloys with nominal Mn concentrations of 85, 70, 65, 60, 55, and 45 wt % were obtained by melting electrolytic Mn and Cu in an induction furnace under an Ar atmosphere. The ingots were homogenized at 850° C for 72 h. The analysed compositions of these alloys are shown in Table I. Homogenized ingots were hot-rolled to 7 and 3 mm thick plates. Samples from these plates were solution treated at 800° C for 2 h and quenched in water at room temperature.

Studies were made under three conditions: alloys at high temperature, quenched alloys, and aged alloys.

The heat-treatment parameters were chosen from dilatometric data [8]. Temperatures of 400, 500, and 600° C were selected for the ageing treatment. An ageing time of 8 h was inferred from the slope of the dilatometric curves.

Microprobe analysis was carried out initially to check the homogeneity of the alloys. All compo-

* Present address: Systems Research Laboratories, Inc, 2800 Indian Ripple Road, Dayton, Ohio 45440, USA.

0022–2461/80/010139–10$03.00/0

TABLE I Chemical analysis of Mn–Cu alloys

Nominal composition wt% Cu	Chemically analysed composition wt% Cu	Alloy composition at% Cu
15	14.65	12.90
30	29.30	26.40
35	36.70	33.40
40	41.20	37.75
45	46.46	42.90
55	54.00	50.40

sitions exhibited good homogeneity. Point analysis was carried out on aged alloys to check for the presence of phases and the composition of the matrix. Optical metallography of these alloys was carried out under solution-treated and aged conditions. Typical optical micrographs of one of the alloys are shown in Fig. 1. Solution-treated alloys up to 50 at% Cu exhibit a single-phase structure. In alloy compositions up to 25 at% Cu, grain-boundary precipitation and needle-shaped precipitates are observed during ageing at 400° C, while at 600° C growth of these precipitates is noticeable. For alloy compositions greater than 25 and less than 50 at% Cu, only grain-boundary precipitates are noticeable during ageing at 400° C. However, needle-shaped precipitates are observed for ageing at 600° C. In the case of an alloy at 50 at% Cu, the presence of grain-boundary precipitates is doubtful after ageing at 400° C; however, after ageing at 600° C, a few precipitates are clearly visible in the structure.

The damping capacity of solution-treated and aged alloys was determined using an Amsler high-frequency vibrophore in conjunction with a drum camera. The specimens, made from 3 mm plates, were subjected to a stress amplitude of 0 ± 4 kg mm^{-2}. The damping values were calculated from the attenuation of vibrations, and the attenuation amplitude was corrected for the damping capacity of the vibrophore itself. Typical damping curves are shown in Fig. 2, and the data are given in Table II. It can be seen from the data that the damping capacity is maximum for the Mn–33.4 at% Cu alloy when aged at 400° C.

2.1. Crystal data

High-temperature (800° C) X-ray diffraction photographs were obtained for these alloys using CuK_α radiation. Thin wire samples, 0.2 mm diameter, were enclosed in quartz capillaries for X-ray exposure. FeK_α radiation was used for obtaining diffraction patterns of the quenched and aged

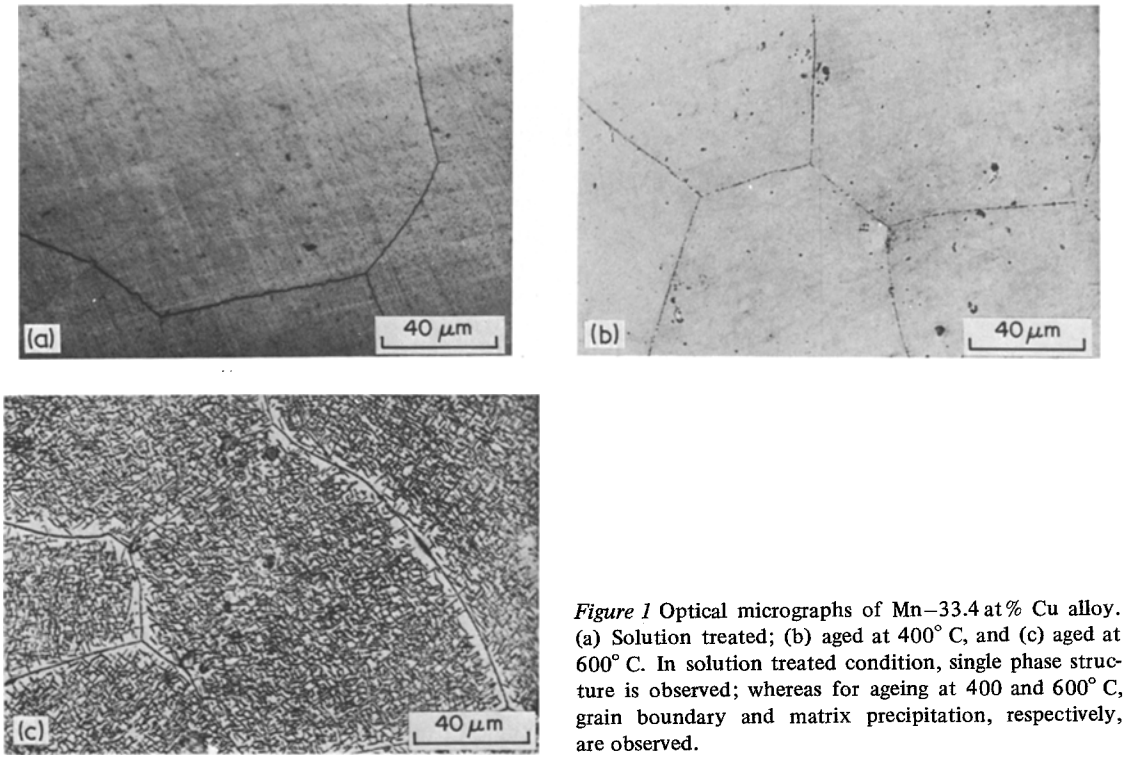

Figure 1 Optical micrographs of Mn–33.4 at% Cu alloy. (a) Solution treated; (b) aged at 400° C, and (c) aged at 600° C. In solution treated condition, single phase structure is observed; whereas for ageing at 400 and 600° C, grain boundary and matrix precipitation, respectively, are observed.

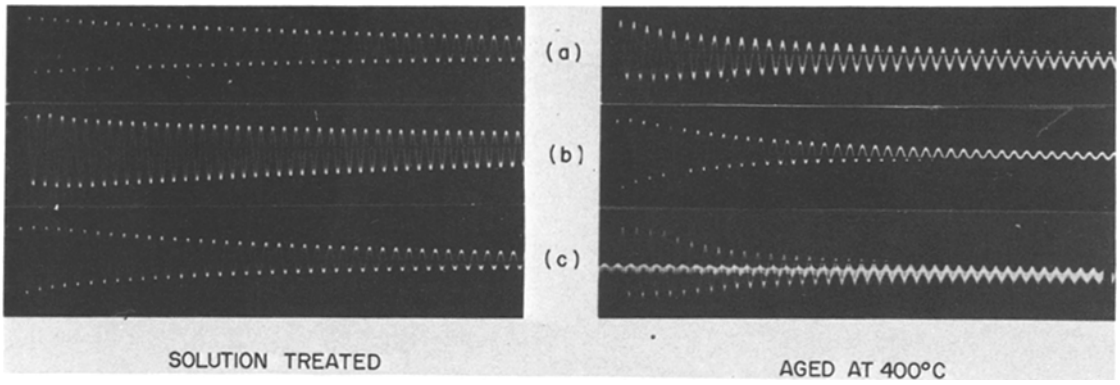

Figure 2 Damping curves for (a) Mn–50.4 at% Cu, (b) Mn–33.4 at% Cu, and (c) Mn–26.4 at% Cu alloys.

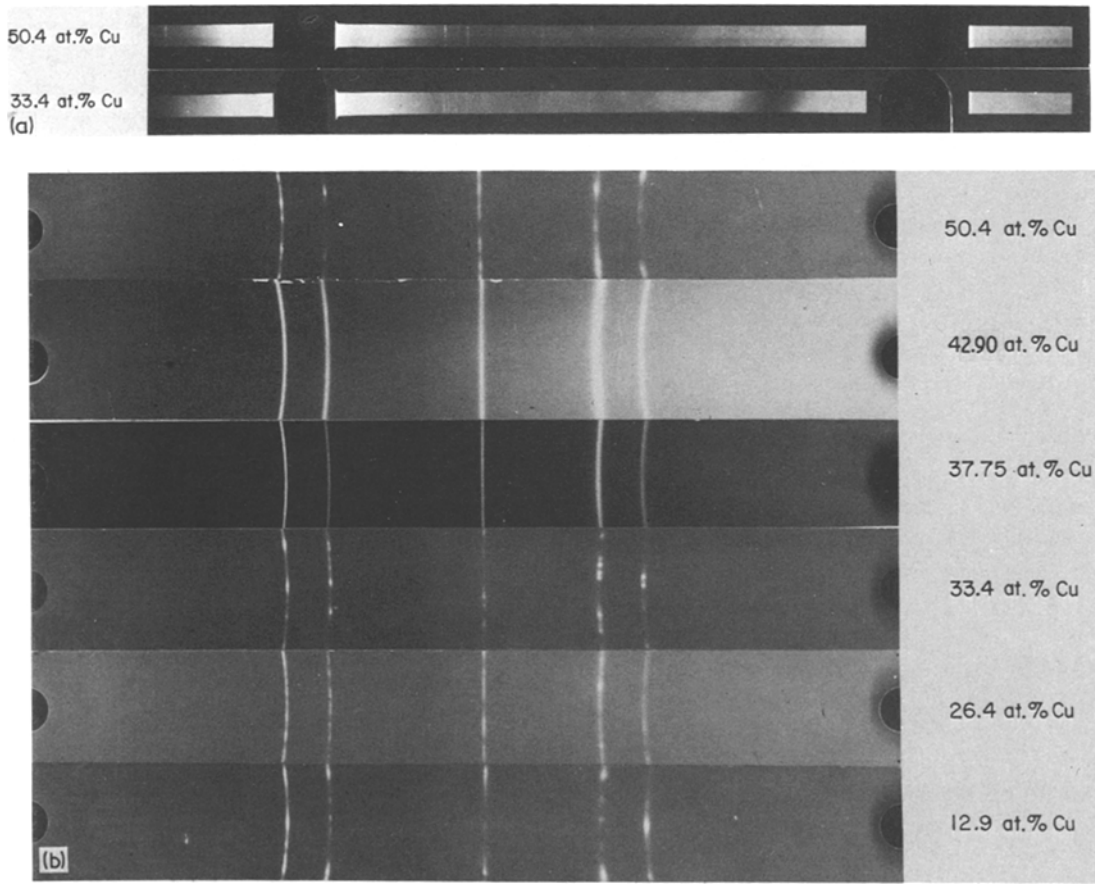

Figure 3 (a) High temperature (800° C) X-ray diffraction photographs of Mn–Cu alloys. (b) X-ray diffraction photographs of quenched Mn–Cu alloys. (c) to (f) X-ray diffraction photographs of Mn–Cu alloys aged at (c) 400° C, (d) 500° C, (e) 600° C, (f) 400° C.

TABLE II Damping capacity of Mn–Cu alloys

Alloy condition	Specific damping capacity		
	50.4 at% Cu	33.4 at% Cu	26.4 at% Cu
Solution treated	28	30	32
Aged at 400° C (10 h)	38	64	28
Aged at 600° C (6 h)	30	22	20

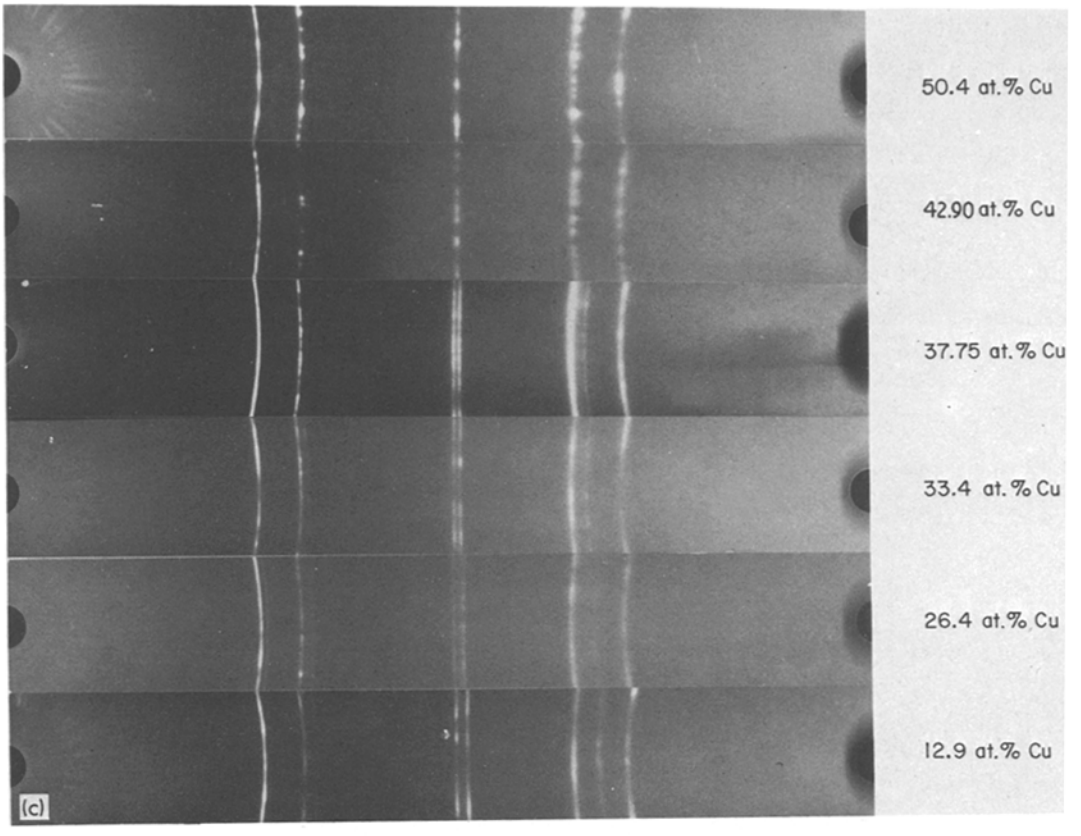

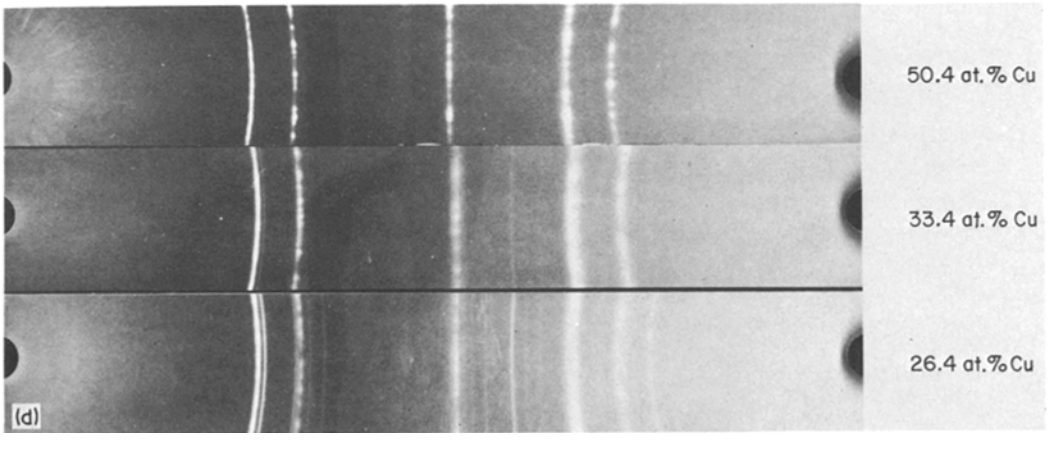

alloys. Powder photographs are shown in Fig. 3, and the diffraction data are given in Table III.

The diffraction patterns at high temperatures do not exhibit variation in d values with increasing Cu concentration up to 50 at% Cu, suggesting that the lattice parameter remains constant throughout the ranges of homogeneity up to 50 at% Cu. A similar observation is also made for the alloys in the quenched condition. The lattice constants are given below.

Alloys at 800° C (up to 50 at% Cu)	Quenched alloys (up to 50 at% Cu)
$a = 2.708$ Å	$a = 2.658$ Å
$b = 8.584$ Å	$b = 11.253$ Å
$c = 11.544$ Å	

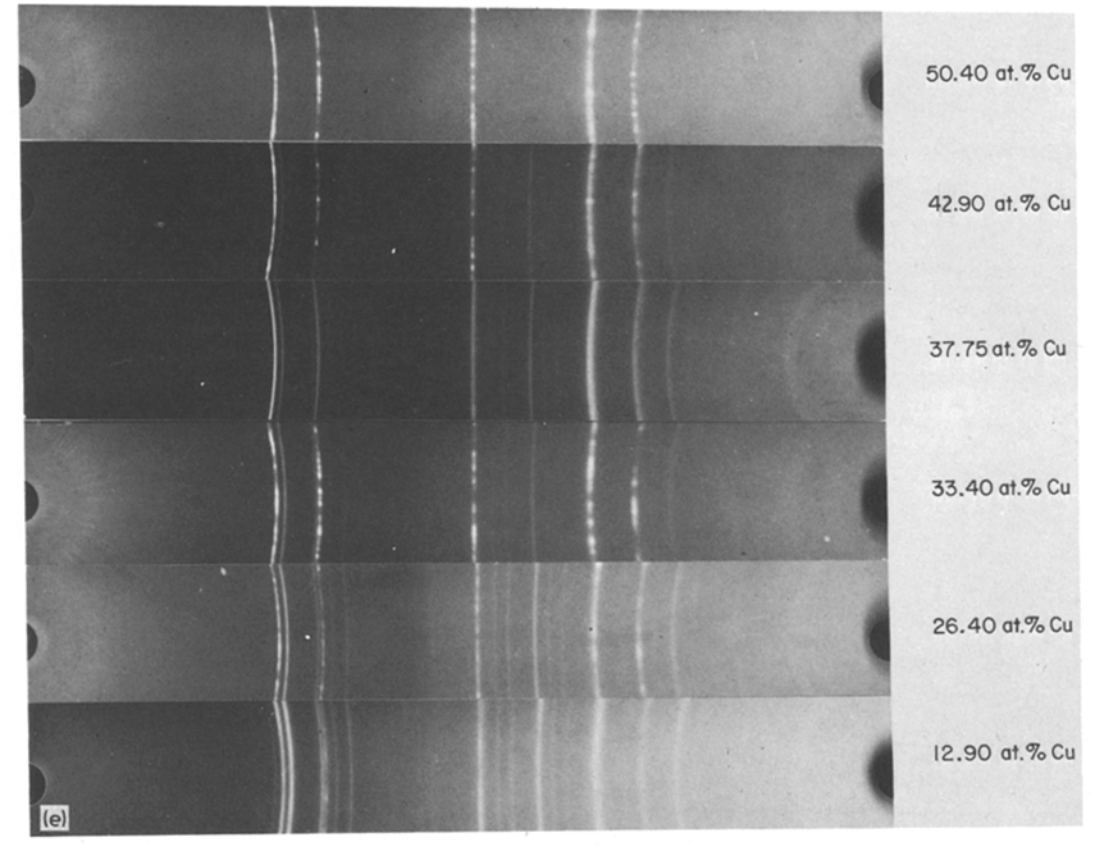

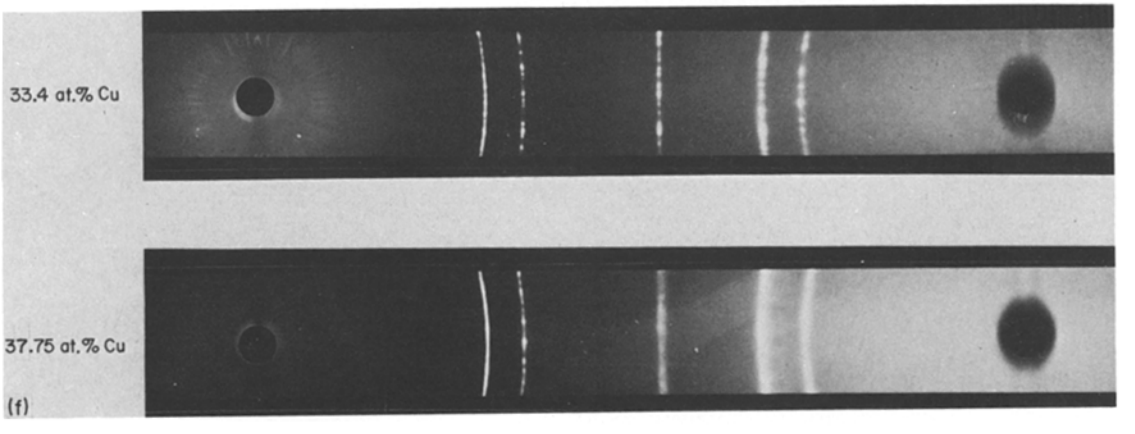

Broad lines having uneven intensity and non-resolution of α_1 and α_2 are noticeable in the X-ray reflections. In some of the patterns for aged alloys, a spotty nature with asymmetric side-bands or saw-tooth [9] line shapes are noticeable. Asterism is also observed in some patterns of aged alloys, as shown in Fig. 3f.

When aged at 400° C, Mn–Cu alloys up to 25 at% Cu exhibit a two-phase structure with α-Mn precipitates in the MnCu matrix. Alloys in the range 25 to 50 at% Cu present variations in the appearance of precipitates and the nature of the matrix. However, for the alloy at 50 at% Cu, only a single-phase structure is observed. The data

TABLE III (a) Crystal data of Mn–Cu alloys at high temperature (800° C)

Mn–50.4 at % Cu *d* values (Å)	Mn–33.4 at % Cu *d* values (Å)	Assigned *h k l*
2.192	2.195	1 0 3
2.141	2.140	0 4 0
2.031	2.035	1 3 0
1.903	1.910	0 0 6
1.870	1.871	0 3 5
1.347	1.352	2 0 0
1.151	1.153	2 1 5
1.105	–	1 6 5, 2 0 6
1.076	–	0 8 0

TABLE III (b) Diffraction data (*d* values in Å) of quenched (from 800° C) Mn–Cu alloys

12.90 at % Cu	26.4 at % Cu	33.4 at % Cu	37.75 at % Cu	42.90 at % Cu	50.40 at % Cu	Assigned indices *h k l*
2.157	2.165	2.165	2.162	2.162	2.165	1 0 3
1.871	1.882	1.881	1.883	1.876	1.882	1 1 0, 0 0 6
1.323	1.328	1.328	1.327	1.327	1.328	1 1 6, 2 0 0
1.129	1.132	1.132	1.132	1.134	1.131	2 1 3
1.081	1.084	1.084	1.086	1.084	1.084	2 0 6

TABLE III (c) Diffraction data (*d* values in Å) of aged Mn–Cu alloys

12.9 at % Cu		26.4 at % Cu		33.4 at % Cu			37.75 at % Cu		42.9 at % Cu		50.40 at % Cu		
400° C	600° C	400° C	600° C	400° C	500° C	600° C	400° C	600° C	400° C	600° C	400° C	500° C	600° C
2.215	2.377	2.210	2.378	*2.156*	2.147	2.375	*2.153*	2.375		2.210	*3.400*		
2.147	2.222	*2.152*	2.224	*1.884*	2.097	2.220	*1.873*	2.220	*2.152*	*2.153*	*2.500*		
2.101	*2.160*	2.097	*2.161*	*1.844*	*1.876*	*2.156*	*2.834*	*2.156*	*1.876*	2.090	*2.156*	*2.161*	*2.185*
1.884	2.096	*1.881*	2.095	*1.334*	1.825	2.096	*1.327*	2.096	*1.832*	1.902	*2.000*	*2.037*	2.115
1.819	1.901	*1.815*	1.902	*1.315*	1.746	1.900	*1.314*	1.900	*1.323*	*1.873*	*1.872*	*1.874*	*2.046*
1.334	*1.872*	1.744	*1.873*	*1.134*	*1.323*	*1.870*	*1.130*	*1.870*	*1.130*	1.822	*1.700*	*1.321*	*1.881*
1.310	1.815	*1.333*	1.814	*1.115*	1.313	1.815	*1.114*	1.815	*1.076*	1.742	*1.323*	*1.129*	*1.327*
1.214	1.751	*1.309*	1.754	*1.079*	1.261	1.748	*1.076*	1.748		1.340	*1.128*	*1.080*	*1.130*
1.134	1.346	1.141	1.347		1.212	1.344		1.344		*1.321*	*1.079*		*1.083*
1.106	*1.323*	*1.131*	*1.324*		*1.129*	*1.321*		*1.321*		1.288			
1.075	1.292	1.104	1.296		1.005	1.288		1.288		1.260			
	1.265	*1.074*	1.267		1.076	1.262		1.262		1.213			
	1.212		1.211		1.052	1.213		1.213		1.193			
	1.197		1.206			1.192		1.192		*1.129*			
	1.130		1.1715			*1.129*		*1.129*		*1.108*			
	1.172		*1.128*			1.107		1.107		*1.052*			
			1.080			*1.082*		*1.082*					
			1.052										
			1.037										

Italic values correspond to matrix.

are given below:

	Up to 25 at% Cu	At 33.4 at% Cu	Beyond > 33.4 at% Cu < to 50 at% Cu	50 at% Cu
MnCu matrix	$a = 2.670$ Å	$a = 2.607$ Å	$a = 2.646$ Å	$a = 2.646$ Å
	$c = 3.654$ Å	$b = 2.678$ Å	$c = 3.664$ Å	$b = 7.938$ Å
	(γ)	$c = 11.004$ Å	(γ)	$c = 3.744$ Å
		(γ')		(γ'')
Precipitate	α-Mn	Not detected	α-Mn	Not detected

When aged at 500° C, these alloys exhibit precipitates of elemental Mn (both α and β forms) up to 50 at% Cu, and precipitates are not detected in the alloy at 50 at% Cu.

When aged at 600° C, all compositions up to 50 at% Cu exhibit elemental Mn precipitates in α-form in the MnCu matrix. However, in the case of the alloy at 50 at% Cu, β-Mn is detected in the matrix. The data are given below:

	< 50 at% Cu	50 at% Cu
MnCu matrix	$a = 2.64$ Å	$a = 2.66$ Å
(γ)	$c = 3.75$ Å	$c = 3.75$ Å
Precipitate	α-Mn	β-Mn

The results obtained in the present study are summarized below to facilitate detailed discussion.

(a) Elemental Mn and Cu form continuous solid solutions up to 50 at% Cu only at high temperatures, beyond 800° C, with orthorhombic structure (b c o). Upon quenching, the structure transforms to tetragonal (b c t).

(b) The lattice parameters of the Mn–Cu alloys (both at high temperature and upon quenching) remain constant with increasing Cu concentrations up to 50 at% Cu.

(c) Quenched alloys upon ageing precipitate elemental Mn in the MnCu matrix. The mode of decomposition of the solid solution and the temperatures at which the decomposition is effected are dependent upon the Cu concentration of the alloys and broadly occur in three stages ($400°\gamma \rightarrow 500°\beta \rightarrow 600°\alpha$) corresponding to the allotropic modification of Mn. The metastable phases determine the boundary of the miscibility gap in the Mn–Cu system.

(d) Upon ageing (400° C) the alloy at Mn–33.4 at% Cu composition develops a high damping capacity.

3. Discussion

The lattice constants (a, b, c) of the high-temperature phase of Mn–Cu alloys, throughout the range of homogeneity, bear the following relation:

$$a \simeq a_0, \quad b \simeq 3a_0 \quad \text{and} \quad c \simeq 3c_0,$$

where a_0 and c_0 refer to a cell of the γ-Mn type (b c t). This suggests that the orthorhombic superstructure of high temperature is formed by the multiplication of cell edges of a basic unit of the type γ-Mn. Since the strain energy resulting from the substitution of atoms having different radii is reduced by multiplication of the cell edges in the alloy superstructure [10], it appears that the atomic radii of Cu and Mn atoms are the controlling factors in the stability of the high-temperature structure. Since Mn atoms have a tendency to exhibit smaller radii and valences while combining with other transition elements [11] and since the multiplication of cell edges occurs in two directions, Mn atoms are considered to have different radii and valences along the crystallographic axes and these fluctuations in radii and valences seem to explain the formation of a continuous series of alloys only at high temperatures. Upon quenching, cell dimensions along two directions become equal, while the multiplication of cell edges along the ⟨0 0 1⟩ direction is retained. It is inferred that the quenching process controls the fluctuations in radii and valences of Mn atoms such that only two types of Mn atoms exist in the tetragonal transformation, rendering it partially ordered. As a consequence of the effect of variable radii and valency, it is seen that as the cell weight (M) increases, the specific volume (σ) of the alloy decreases, thereby making $M\sigma$ constant. This consideration at high temperatures and upon quenching seems to explain the constancy of the lattice parameter with an increase in Cu concentration. This suggests that Mn–Cu alloys upon quenching undergo an unusual transformation associated with fluctuations in valency and radii of the Mn atoms in the alloy structures. These observations are in conformity with dilatometric data [8] in that volume changes occur during heat treatment of the quenched Mn–Cu alloys.

It is also seen from the crystal data that through-

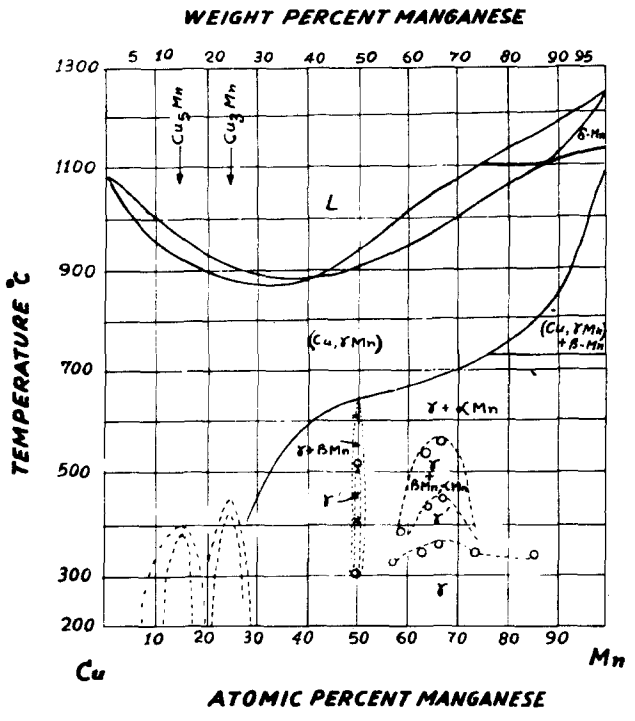

Figure 4 Phase diagram of Mn–Cu alloy system incorporating the results of the present study.

out the range, the superstructure both at high temperature and under quenched conditions is based upon a γ-Mn type basic lattice with two atoms per unit cell having approximately MnCu stoichiometry. It is, therefore, inferred that Mn–Cu alloys (up to 50 at% Cu) form an equi-atomic metastable phase field in which Mn atoms exhibit variable valency in the same structure. Depending upon the Cu concentration, Mn-rich alloys corresponding to $Mn_{2-x}Cu_x (x \leqslant 1)$ stoichiometry are obtained. When $x = 0.25$, 0.333, 0.50, 0.66, and 1.00, the metastable alloys have the formulae Mn_7Cu, Mn_5Cu, Mn_3Cu, Mn_2Cu, MnCu. During heat treatment, the variable valency of Mn atoms creates environments of like and unlike Mn atoms in the structure, resulting in the variable solubility of Cu in $Mn_{2-x}Cu_x$ alloys. Quenched solid solutions, therefore, decompose and elemental Mn is precipitated in the equi-atomic MnCu matrix. During the early stages (at 400° C), an environment of unstable elemental γ-Mn separates out, which finally transforms to stable α-Mn. The formation of like and unlike Mn atoms and subsequent transformation of elemental Mn ($400 \underrightarrow{\gamma} 500 \underrightarrow{\beta} 600 \underrightarrow{\alpha}$) is

TABLE IV Outline of the miscibility gap in Mn–Cu system

	Alloy at% Cu	Temperatures within miscibility gap	Temperatures outside miscibility gap
I	12.9	Below 340° C (γ)	Above 340° C
II	26.4	Below 380° C (γ)	Above 380° C
III	33.4	Below 350° C (γ) 350–450° C (γ′) 450–560° C (γ + βMn, αMn)	560° C and above
IV	37.75	Below 340° C (γ) 340–425° C (γ′) 425–530° C (γ + βMn, αMn)	530° C and above
V	42.9	Below 320° C (γ) 320–375° C (γ + βMn, αMn)	375° C and above
VI	50.40	Below 300° C (γ) 300–525° C (γ″) Above 525° C (γ + βMn, αMn)	

very rapid up to 25 at% Cu and becomes sluggish as the Cu concentration is increased up to 50 at% Cu. In all alloys, an equi-atomic MnCu matrix is obtained after the precipitation of stable α-Mn. It is, therefore, concluded that Mn–Cu alloys throughout the range of homogeneity up to 50 at% Cu are in the extended range of solid solubility beyond the equi-atomic composition and the miscibility gap and that the metastable phases are related to the allotropic modification of elemental Mn beyond the limit of solid solubility at 50 at% Cu. These details are shown in Fig. 4 and Table IV.

Since it is known [12] that for a two-component system, if the terminal solid solubility is limited, there is a range of compositions beyond the equilibrium solubility limit of the alloy in which alloy films having metastable structures of terminal solid solutions are formed, it appears (by close analogy) that Mn-rich alloys of the Mn–Cu system produce metastable phases having abnormal structures in this solubility range beyond equilibrium solubility. The extent of this range (i.e. extended range of solid solubility) is determined by the ratio of atomic radii of the component, i.e. Mn and Cu. Moreover, Mn–Cu alloys undergo an unusual transformation upon quenching and form an abnormal intermetallic compound structure during heat treatment. The first stage commences at $0.3\,T_m$; and the final stage ends at $0.5\,T_m$, where T_m is the average of the melting points of the components in K. Therefore, it is concluded that Mn–Cu alloys undergo a transformation resulting in the formation of an abnormal metastable structure throughout the range of homogeneity up to 50 at% Cu concentration.

In the case of the $Mn_{2-x}Cu_x$ alloy at $x = 0.666$, the composition has the formula Mn_2Cu with $Z = 2$ in the b c t structure and corresponds to the centre of the miscibility gap. During heat treatment around $0.3\,T_m$ (400° C), the process of creating like and unlike Mn atoms (in excess of equi-atomic composition) which retain the MnCu matrix is accompanied by separation of γ-Mn having the bct structure. Since the elemental γ-Mn together with the MnCu phase describes a superstructure, it is considered that constrained γ-Mn exists in the compound structure. This 2D-structure creates a misfit at interfaces, thereby developing lattice strain in the matrix (Fig. 5). The response of this lattice strain to the externally applied stress is thought to be responsible for high damping in this alloy.

During finalisation of our results in the present study, investigations by Vintaykin *et al.* [13] and

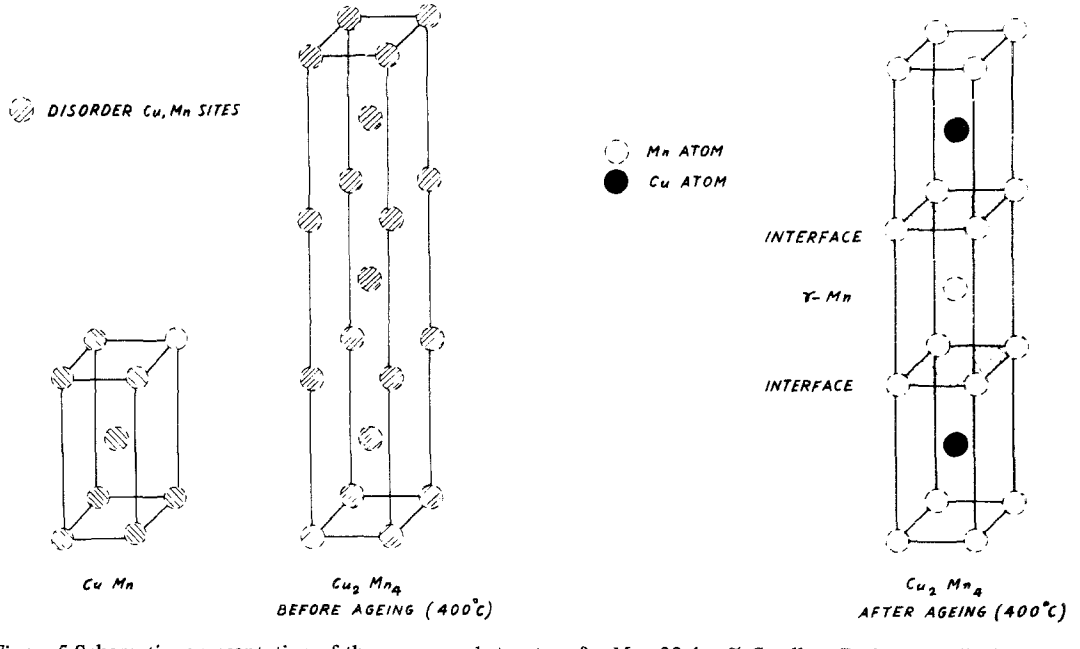

Figure 5 Schematic representation of the compound structure for Mn–33.4 at% Cu alloy. Basic unit cell of MnCu phase where atom sites are occupied randomly by Cu and Mn atoms. The quenched alloy derives a cell structure based upon MnCu unit cell, and the multiplication of cell edges in ⟨0 0 1⟩ direction is shown. The aged (at 400° C) alloy assumes a compound structure of CuMn where the atom positions are non-random. The proposed "interface" between MnCu and γ-Mn phases in the structure is shown.

Vitek and Warlimont [14] were published in which the metastable miscibility gap in this system was described. The miscibility curve outlined by Vintaykin *et al.* was based upon their limited experimental data from neutron scattering; and the observation of Vitek and Warlimont was based upon experimental data from hardness measurements on these alloys. The miscibility curves outlined by these authors do not agree amongst themselves and also with that outlined in this study. In the present study, the maximum point in the miscibility curve which occurred at 33.4 at% Cu is in close agreement with that of Vintaykin *et al.*; however, the temperature of occurrence of this maximum does not agree. The curve proposed by Vitek and Warlimont is displaced toward a lower Cu concentration (≈ 20 at%), although the temperature for the maximum in the curve agrees well with that in the present study. The variation of location and the temperature of the maximum in the miscibility curves in all these studies may be attributed to possible variations in the quenching rate adopted by different workers.

4. Conclusions

(1) Mn–Cu alloys form a series of Mn-rich solid solutions at higher temperature and have a range of homogeneity up to 50 at% Cu which is the limiting solid solubility. Alloys up to 50 at% Cu (equi-atomic) are in the extended range of homogeneity and form the $Mn_{2-x}Cu_x$ phase ($x \leqslant 1$). The lattice parameters of the alloys remain constant throughout the range of homogeneity.

(2) During quenching, Mn–Cu alloys undergo an unusual phase transformation associated with the variable valency of Mn-atoms and form a family of partially ordered tetragonal structures. The lattice parameters of the quenched alloys remain constant throughout the range of homogeneity and abnormal metastable structures are formed.

(3) Aged Mn–Cu alloys undergo phase transformations in three temperature ranges. The temperatures of transformation determine and describe the miscibility gap at lower temperatures. The stability of aged alloys in the MnCu phase field depends upon the allotropic form of the elemental Mn beyond the equi-atomic stoichiometry. The rapidity or sluggishness of transformation of γ-Mn beyond the equi-atomic stoichiometry depends upon the Mn : Cu ratio in the $Mn_{2-x}Cu_x$ phase.

(4) Strain energy corresponding to the variable radii and valence of Mn is the controlling factor in the alloying behaviour of γ-Mn in the $Mn_{2-x}Cu_x$ phase.

(5) In the $Mn_{2-x}Cu_x$ phase when $x = 0.666$, the alloy corresponds to the centre of the miscibility gap and exhibits the highest damping capacity. High damping in this system is considered to be a transient phenomenon and can be observed until γ-Mn (beyond equi-atomic stoichiometry) ceases to change to other allotropic forms.

Acknowledgements

The authors wish to thank Marian Whitaker and Helen Bailey for editorial assistance and preparation of the manuscript, and the Director, DMRL, for permission to publish this paper. Thanks are also due to Dr R. Krishnan of BARC, Bombay, for help with the high temperature X-ray diffraction work.

References

1. J. A. HEDLEY, *Met. Sci. J.* **2** (1968) 129.
2. D. BIRCHON, D. E. BROMLEY and D. HEALEY, *ibid* **2** (1968) 41.
3. R. J. GOODWIN, *ibid* **2** (1968) 121.
4. S. DEAN, "Electrolytic Manganese and Its Alloys" (Ronald Press, New York, 1952).
5. A. H. SULLY, "Manganese" (Butterworths, Wobern, Mass., 1955).
6. ASTM Card No. 17-190, γ-Manganese.
7. F. A. SHUNK, "Constitution of Binary Alloys", Second Supplement (McGraw-Hill, New York, 1969).
8. P. VENKATESWARARAO and D. K. CHATTERJEE, "Thermal Expansion and Temperature Capability of Mn–Cu Alloys". Unpublished work: DMRL internal report.
9. G. L. CLARK, "The Encyclopedia of X-Rays and Gamma Rays" (Reinhold, New York, 1963) p. 732.
10. W. B. PEARSON, "The Crystal Chemistry and Physics of Metals and Alloys" (Wiley, New York, 1972).
11. P. A. BECK, "Electronic Structure and Alloy Chemistry of the Transition Elements" (Interscience, New York, 1963).
12. K. L. CHOPRA, "Thin Film Phenomena" (McGraw-Hill, New York, 1969).
13. YE. Z. VINTAYKIN, D. F. LITVIH and V. A. UDOVENKO, *Fiz. Metal Metalloved* **37** (1974) 1228.
14. J. M. VITEK and H. WARLIMONT, *Met. Sci. J.* **1** (1976) 7.

Received 26 April and accepted 28 June 1979.